



RESEARCH ARTICLE

Comprehensive molecular and clinicopathological analysis of vascular malformations: A study of 319 cases

Roel W. Ten Broek^{1†}  | Astrid Eijkelenboom^{1†} | Carine J. M. van der Vleuten^{2,3} |
 Eveline J. Kamping⁴ | Marleen Kets^{4,3} | Bas H. Verhoeven^{5,3} | Katrien Grünberg¹ |
 Leo J. Schultze Kool^{6,3} | Bastiaan B. J. Tops⁷ | Marjolijn J. L. Ligtenberg^{1,4†} | Uta Flucke^{1,7,3†} 

¹Department of Pathology, Radboud University Medical Center, Nijmegen, The Netherlands

²Department of Dermatology, Radboud University Medical Center, Nijmegen, The Netherlands

³Radboudumc Expertise Center for Hemangiomas and Congenital Vascular Anomalies Nijmegen (Hecovan), Radboud University Medical Center, Nijmegen, The Netherlands

⁴Department of Human Genetics, Radboud University Medical Center, Nijmegen, The Netherlands

⁵Department of Surgery, Radboud University Medical Center, Nijmegen, The Netherlands

⁶Department of Radiology and Nuclear Medicine, Radboud University Medical Center, Nijmegen, The Netherlands

⁷Princess Máxima Center for Pediatric Oncology, Utrecht, The Netherlands

Correspondence

Uta Flucke, Radboud University Medical Center, Department of Pathology, P.O. Box 9101, 6500 HB Nijmegen, The Netherlands.
 Email: uta.flucke@radboudumc.nl

Abstract

Vascular malformations are part of overgrowth syndromes characterized by somatic mosaic mutations or rarely by germline mutations. Due to their similarities and diversity, clinicopathological classification can be challenging. A comprehensive targeted Next Generation Sequencing screen using Unique Molecular Identifiers with a technical sensitivity of 1% mutant alleles was performed for frequently mutated positions in ≥ 21 genes on 319 formalin-fixed paraffin-embedded samples. In 132 out of 319 cases pathogenic mosaic mutations were detected affecting genes previously linked to vascular malformations e.g. *PIK3CA* (n=80), *TEK* (*TIE2*) (n=11), *AKT1* (n=1), *GNAQ* (n=7), *GNA11* (n=4), *IDH1* (n=3), *KRAS* (n=9), and *NRAS* (n=1). Six cases harbored a combination of mutations in *PIK3CA* and in *GNA11* (n=2), *GNAQ* (n=2), or *IDH1* (n=2). Aberrations in *PTEN* and *RASA1* with a variant allele frequency approaching 50% suggestive of germline origin were identified in six out of 102 cases tested; four contained a potential second hit at a lower allele frequency. Ninety-one of the total 142 pathogenic mutations were present at a variant allele frequency <10% illustrating the importance of sensitive molecular analysis. Clinicopathological characteristics showed a broad spectrum and overlap when correlated with molecular data. Sensitive screening of recurrently mutated genes in vascular malformations may help to confirm the diagnosis and reveals potential therapeutic options with a significant contribution of *PIK3CA*/mTOR and RAS-MAPK pathway mutations. The co-existence of two activating pathogenic mutations in parallel pathways illustrates potential treatment challenges and underlines the importance of multigene testing. Detected germline mutations have major clinical impact.

KEYWORDS

molecular genetics, mosaic mutations, overgrowth syndromes, vascular malformations

1 | INTRODUCTION

Somatic overgrowth syndromes encompass entities with predominant vascular malformations on the one hand and conditions with more pronounced overgrowth of tissue with only a limited vascular component on the other hand.^{1–4} This spectrum of lesions is characterized by pathogenic somatic mosaic mutations resulting in a variable

clinicopathological presentation.⁵ Most of these mutations are activating in genes related to cell growth, proliferation, survival, and cell cycle progression.⁶ In comparison with rare familial vascular malformation syndromes that occur with typical patterns of inheritance,⁷ sporadic cases are more common.⁸

Recurrently mutated genes were identified in several vascular anomalies including overgrowth/vascular malformation syndromes like *PIK3CA*-related overgrowth syndrome (PROS),^{2,8–11} Proteus syndrome (activating mutations in *AKT1*),¹² Sturge Weber syndrome

† Authors contributed equally.

(activating mutations in *GNAQ*)¹³ and Maffucci syndrome (transforming mutations in *IDH1* and *IDH2*).¹⁴

Other somatically mutated genes comprise *TEK/TIE2* (activating mutations, mainly described in venous malformations),⁸ *KRAS*, *NRAS*, and *HRAS* (activating mutations, mainly described in arteriovenous malformations),^{15,16} *GLMN* (disrupting mutations in glomovenous malformations)¹⁷ and *GNA11* and *GNA14* (activating mutations in vascular lesions described as vascular tumors including congenital tufted angiomas and kaposiform hemangioendotheliomas).¹⁸

Germline *RASA1*-mutations have been described in patients with Parkes Weber Syndrome and Capillary Malformation-ArterioVenous Malformations (CM-AVM).^{19,20} The *PTEN* Hamartoma Tumor Syndrome includes Bannayan-Riley-Ruvalcaba syndrome (BRRS) and Cowden syndrome (CS) harboring disrupting (germline) mutations in *PTEN*.^{21,22} Hereditary hemorrhagic telangiectasia bears disrupting germline mutations in *ENG* and *ACVRL1*.¹⁹ Other known syndromes and disorders that may include vascular anomalies are Beckwith-Wiedemann syndrome, Noonan syndrome, Turner's syndrome, Klinefelters syndrome, and Neurofibromatosis.¹

To gain better insight into the biology of vascular malformations and overgrowth syndromes, their mutational spectrum and potential therapeutic options, we performed Next Generation Sequencing (NGS) analysis with a sensitivity of 1% variant allele frequency to allow detection of low abundant mosaic mutations in formalin-fixed paraffin-embedded (FFPE) tissue from 319 clinical cases.

2 | MATERIALS AND METHODS

The 319 included cases are combined from a prospective and a retrospective cohort. The prospective samples ($n = 217$) were from routine diagnostics. The retrospective samples, ($n = 102$) retrieved from our pathology files, were all histologically reviewed and if possible, clinically and radiologically confirmed as vascular malformation according to the INTERNATIONAL SOCIETY FOR THE STUDY OF VASCULAR ANOMALIES (ISSVA) classification. In a few cases a somatic overgrowth syndrome (SOGS) without a prominent vascular component was diagnosed. The study was conducted in accordance with the Code of Conduct of the Federation of Medical Scientific Societies in the Netherlands after consent of the internal ethical review board (2016-2310).

All samples were fixed in 4% buffered formalin, routinely processed and embedded in paraffin. Four micrometer thick sections were stained with hematoxylin and eosin.

DNA isolation and library preparation were performed as previously described.^{23,24} Briefly, gDNA was isolated from FFPE tissue sections (generally $3 \times 20 \mu\text{m}$) using 5% Chelex-100 and 400 μg proteinase K and DNA concentrations were measured using the Qubit Broad Range kit (Q32853; ThermoFisher). When available, 150 ng of gDNA representing an equivalent of ~25 000 cells was used per library preparation. In the remaining cases, the available amount of DNA was used with a minimum of 5 ng representing gDNA from approximately 800 cells.

Libraries for sequencing on the NextSeq 500 (Illumina) were generated using Single Molecule Molecular Inversion Probes (smMIPs).²⁴ This method uses unique molecule identifiers (UMI's) to

allow consensus-based error correction and the deduction of the actual number of sequenced gDNA molecules. Variant calling required detection of ≥ 3 mutant gDNA molecules representing a minimum of 1% of the total unique coverage. The strand-specific nature allows the distinction between deamination artifacts from genuine C:G > T:A mutations.²⁴ This method therefore allows both sensitive detection of variants down to 1% variant allele frequency and specification of the sensitivity of sequencing on a case-by-case basis.

The prospective cohort was analyzed using a panel targeting the following "cancer" hotspots and surrounding sequences (the exact positions analyzed for variants are shown in Eijkelenboom et al²⁴): *AKT1* (NM_005163.2): codon 17; *BRAF* (NM_004333.4): codon 582-615; *CTNNB1* (NM_001904.3): codon 19-48; *EGFR* (NM_005228.3): codon 465-499, 688-823, 849-875; *ERBB2* (NM_004448.3): codon 770-785; *GNA11* (NM_002067.4): codon 183 and 209; *GNAQ* (NM_002072.3): codon 183 and 209; *GNAS* (NM_000516.4): codon 201 and 227; *H3F3A* (NM_002107.4): codon 28 and 35; *H3F3B* (NM_005324.4): codon 37; *HRAS* (NM_005343.2): codon 12, 13, 59 and 61; *IDH1* (NM_005896.3): codon 132; *IDH2* (NM_002168.3): codon 140 and 172; *JAK2* (NM_004972.3): codon 617; *KIT* (NM_000222.2): codon 412-513, 550-591, 628-713, 799-828; *KRAS* (NM_004985.4): codon 12, 13, 59, 61, 117 and 146; *MPL* (NM_005373.2): codon 515; *MYD88* (NM_002468.4): codon 265; *NRAS* (NM_002524.4): codon 12, 13, 59, 61, 117 and 146; *PIK3CA* (NM_006218.2): codon 520-554, 1020-1069; *PDGFRA* (NM_006206.4): codon 552-596, 632-667, 814-848.²⁴

For the retrospective cohort our panel was supplemented with *GNA14* (NM_004297.3) codon 205, 206; *PIK3CA* (NM_006218.2): codon 420 and *TEK* (NM_000459.4) codon 897, 915-920, 925, 1100; exons 3 and 13 of *GLMN* (NM_053274); *PTEN* (NM_000314), *RASA1* (NM_002890), *ACVRL1* (NM_000020) and *ENG* (NM_001114753) (smMIP sequences of these genes are shown in Supporting Information Table S1).

We excluded cases without identified (likely) pathogenic mutations if less than 125 individual genomic DNA (gDNA) molecules were analyzed at the frequently mutated positions. For NGS analyses above this threshold, the presence of mutations with an allele frequency > 5% could be excluded with 95% confidence.²⁴ A total of 286 cases (89.6%) fulfilled these requirements for reliable analysis.

No informed consent for the possibility of detecting germline mutations (*PTEN*, *RASA*, and *TEK*) was obtained for the retrospective cohort. Data could therefore only be analyzed anonymously at the group level. Based on very low variant allele frequencies in our *TEK* positive cases (all 12% or lower [see Table]) none of the identified variants were likely germline mutations. As a consequence, we repeated the analyses for *GNA11*, *GNAQ*, *KRAS*, and *TEK* mutated cases to correlate phenotype and genotype. To increase the size of the anonymous group we also excluded the 27 *PIK3CA*-mutated cases because clinical (and histopathological) characteristics are well-studied.^{25,26}

Genetic data from our entire prospective cohort were correlated with clinical and histopathological features.

3 | RESULTS

3.1 | Molecular results

The identified pathogenic and likely pathogenic variants are listed in Table 1 and Supporting Information Table S2 (all *PIK3CA* mutated cases).

3.1.1 | The spectrum of gain of function (hotspot mutations)

Prospective cohort

Nineteen out of 217 prospective cases obtained insufficient coverage. Of the remaining 198 cases, 77 had mutations: 53 *PIK3CA*, 6 *GNAQ*, 6 *KRAS*, 3 *IDH1*, 3 *GNA11*, 1 *NRAS*, and 1 *AKT1* pathogenic mutations. Four cases harbored two mutations: *PIK3CA* and *GNA11* ($n = 2$), *PIK3CA* and *GNAQ*, and *PIK3CA* ($n = 1$) and *IDH1* ($n = 1$).

Retrospective cohort

In the retrospective cohort ($n = 102$), 14 samples were excluded due to insufficient coverage. Among the remaining 88 cases, 45 cases had mutations: 27 *PIK3CA*, 11 *TEK* (one with two mutations in *cis*, *TEK*: c.[2690A > G; c.2752A > G], p.[Tyr897Cys; Arg918Cys]), three *KRAS*, one *GNAQ* and one *GNA11* hotspot mutation. There was one case with double-mutations in *PIK3CA* and *GNAQ* and one affecting *PIK3CA* and *IDH1*. Mutations and histological types of both cohorts are shown in Figure 1.

Overall, we discovered gain of function (hotspot) mutations in a total of 122 cases (43%), with allele frequencies ranging from 2% to 24%. The mutant allele frequencies of 72% of cases ($n = 88$) were below the presumed detection limit of 10% for Sanger and first generation NGS approaches (Figure 2). Six of all mutated cases (5%) harbored a combination of known pathogenic mutations in *PIK3CA* with mutations in *GNA11*, *GNAQ*, or *IDH1* with comparable mutant allele frequencies (Figure 3).

3.1.2 | Loss of function mutations

In addition to the mutations investigated earlier, the retrospective cohort ($n = 88/102$) was analyzed for loss of function mutations in *PTEN*, *RASA1*, *ACVRL1*, *ENG*, and relevant exons of *GLMN*. We identified pathogenic loss of function mutations in *PTEN* (9 cases) and *RASA1* (1 case) (Figure 4), mutually exclusive with the earlier described hotspot mutations. Six cases had mutant allele frequencies >40%. Because the tissue selection for DNA isolation in these cases was identical to the other cases in the cohort and mutant allele frequencies >40% were not identified for any of the other genes, this was interpreted as being germline variants in one *RASA1* positive case and at least 4 out of 9 *PTEN* positive cases. In 3 of these 6 cases with a variant allele frequency >40% a potential second hit was observed at a lower allele frequency ($\leq 10\%$), indicative of a combination of a germline pathogenic mutation with a mosaic second hit. In the fifth possible *PTEN* germline case, the variant allele frequency of 71% suggested loss of the wild type allele and thus complete loss of a functional *PTEN* copy in a subset of cells. We did not find any pathogenic inactivating variants in *GLMN*, *ENG*, and *ACVRL1*, making the presence of mutations less likely, although horizontal and vertical coverage may have

been insufficient to exclude low mosaic mutations (unique coverage of both activating and inactivating genes is shown in Supporting Information Tables S3 and S4). Also unique coverage of *RASA1* was insufficient to exclude the presence of mutations in other cases.

3.2 | Clinical data

The *PIK3CA* mutated lesions were mainly low flow (lymphatic and/or venous) malformations, but comprised heterogeneous clinical aspects as reported in the literature.^{2,25,26} Three patients had clinical characteristics of Klippel Trenaunay syndrome (Table 1).

The clinical data of the 42 cases harboring hotspot mutations other than *PIK3CA* are shown in Table 1. Briefly, 21 patients were female and 21 were male aged between 2 and 81 years (median 35 years and mean 38 years). Patients had diverse clinical presentations with lesions arising at various anatomical sites with most of them localized in the subcutis/skin ($n = 30$). Other lesions were located in soft tissue ($n = 6$), bone ($n = 3$), (epi)dural ($n = 2$), and intracerebral ($n = 1$). Two patients had a vascular malformation associated with other anomalies in the context of Proteus ($n = 1$), and Sturge Weber syndromes ($n = 1$). The case with a double mutation in *TEK* clinically fitted well with a Blue Rubber Bleb Nevus (BRBN) syndrome.

Of the cases with double mutations, the first case with a *PIK3CA* and *GNAQ* mutation was an intraosseous/dural vascular lesion and the second case was a small relatively well-circumscribed high flow skin lesion. One of the two cases with both a *PIK3CA* and a *GNA11* mutation concerned a low flow lesion in the nose with bleeding. The clinical information of the other case was unknown. Finally, the two cases with both a *PIK3CA* and an *IDH1* mutation were both clinically atypical vascular skin lesions localized on the site of the scapula and the leg, respectively. Overall, these 6 cases had no special clinical signs indicating their double mutations.

Reasons for obtaining tissue were also diverse. In 13 patients a diagnostic biopsy was taken for genetic analysis. In 17 cases tissue was surgically removed for various reasons: for correction ($n = 7$), to reduce pain ($n = 3$), and because of progression ($n = 5$) involving one case with paraplegia due to an epidural mass and twice an amputation of a lower leg and a finger, respectively. Other reasons were treatment of varicosity, phlebitis, and a debulking resection because of a massive lesion in the upper lip. Only sparse clinical information was available for 12 patients.

3.3 | Correlation of histology and molecular findings

The *PIK3CA* mutated cases depicted variable histology ranging from simple to combined capillary, lymphatic, and venous malformations and AVMs. All 11 cases with activating mutations in *TEK* were noncircumscribed mostly combined venous, capillary, and/or lymphatic lesions without an arterial component. Eight of the eleven cases with *RAS* (9 *KRAS*, 1 *NRAS*, and 1 *RASA1*) mutations were well-circumscribed capillary and/or venous/cavernous malformations (Figure 5). The remaining 2 cases were noncircumscribed AVMs (Figure 6). Two of three cases with an *IDH1* mutation, were typical spindle cell hemangiomas (SCH) and the third sample showed an intramuscular veno-capillary malformation. All 4 *GNA11* mutated cases had

TABLE 1 Clinical information and all (likely) pathogenic mutations and mutant allele frequencies identified in the prospective and retrospective cohorts are listed (with the exception of the 80 *PIK3CA* mutations, see Supporting Information Table S1)

Gene	Identified variant(s)	Variant allele frequency (%)	Age/sex	Site	Clinical features	Histology
Prospective panel						
<i>GNA11</i>	c.627G > C (p.Gln209His)	9	64/m	Hand	Unknown	Veno-capillary malformation
<i>GNA11</i>	c.547C > T (p.Arg183Cys)	5	61/m	Upper eyelid	Congenital port wine stain; progressive hypertrophy	Veno-capillary malformation
<i>GNA11</i>	c.626A > T (p.Gln209Leu)	3	72/m	Acetabulum	Unknown	Veno-capillary malformation
<i>GNAQ</i>	c.548G > A (p.Arg183Gln)	8	67/f	Skin neck	Residue after venous malformation	Veno-capillary malformation
<i>GNAQ</i>	c.627A > C (p.Gln209His)	4	57/f	Arm	Atypical lesion; spectrum non-involuting congenital hemangioma (NICH)/venous malformation	Veno-capillary malformation
<i>GNAQ</i>	c.548G > A (p.Arg183Gln)	8	81/f	Lower lip	Port wine stain in Sturge Weber Syndrome	Combined vascular malformation
<i>GNAQ</i>	c.627A > C (p.Gln209His)	18	64/f	Epidural	Epidural mass	Veno-capillary malformation
<i>GNAQ</i>	c.548G > A (p.Arg183Gln)	8	43/f	Upper lip	Port wine stain with firm hypertrophy; KTS spectrum	Venous malformation
<i>GNAQ</i>	c.626A > T (p.Gln209Leu)	21	15/m	Skin clavicle	Non congenital vascular high flow lesion	Veno-capillary malformation
<i>AKT-1</i>	c.49G > A (p.Glu17Lys)	8	5/m	Saphenous vein	Congenital port wine stain of one leg with firm overgrowth; mild phenotype of Proteus.	Venous malformation
<i>KRAS</i>	c.35_38delinsCTCA (p.Gly12_Gly13delinsAlaHis)	32	56/f	Flank	Vascularized tumor	Veno-capillary malformation
<i>KRAS</i>	c.64C > A (p.Gln22Lys)	22	32/m	Cheek	KTS-spectrum with lymphedema and port-wine stain leg and multiple vascular lesions left side face	Veno-capillary malformation
<i>KRAS</i>	c.35G > C (p.Gly12Ala)	18	32/m	Cheek	Lipoma with vascular lesion	Venous malformation
<i>KRAS</i>	c.436G > A (p.Ala146Thr)	17	45/f	Arm	KTS spectrum with venolymphatic lesion and port wine stain	Venous malformation
<i>KRAS</i>	c.37G > T (p.Gly13Cys)	2	8/f	Lower jaw	Unknown	Veno-capillary malformation
<i>KRAS</i>	c.35G > A (p.Gly12Asp)	9	70/f	Subcutis buttock	Unknown	Veno-capillary malformation
<i>NRAS</i>	c.182A > G (p.Gln61Arg)	14	12/m	Thoracal skin	Multiple eruptive pyogenic granuloma	Capillary malformation
<i>IDH1</i>	c.394C > T (p.Arg132Cys)	2	12/f	Upper arm muscle	Venous malformation or non-involuting congenital hemangioma	Veno-capillary malformation
<i>IDH1</i>	c.394C > T (p.Arg132Cys)	14	38/f	Foot	Unknown	SCH
<i>IDH1</i>	c.394C > T (p.Arg132Cys)	10	15/m	Soft tissue foot	Unknown	SCH
<i>PIK3CA; GNAQ</i>	c.3140A > G (p.His1047Arg); c.627A > C (p.Gln209His)	26; 26	53/m	Skull/dura	Vascular proliferation with Masson-like features	Veno-capillary malformation
<i>PIK3CA; GNA11</i>	c.3140A > G (p.His1047Arg); c.627G > C (p.Gln209His)	17; 17	57/m	Skin pericumbilical	Unknown	Veno-capillary malformation
<i>PIK3CA; GNA11</i>	c.1633G > A (p.Glu545Lys); c.627G > T (p.Gln209His)	7; 6	45/m	Skin nose	Venous malformation	Veno-capillary malformation
<i>PIK3CA; IDH1</i>	c.3140A > G (p.His1047Arg); c.394C > T (p.Arg132Cys)	12; 9	5/f	Scapula	Venolymphatic malformation, atypical by ultrasound	SCH

(Continues)

TABLE 1 (Continued)

Gene	Identified variant(s)	Variant allele frequency (%)	Age/sex	Site	Clinical features	Histology
Retrospective panel						
TEK	c.2690A > G (p.Tyr897Cys)	3	11/f	Jaw	Venous malformation	Venous malformation
TEK	c.2740C > T (p.Leu914Phe)	5	20/f	Labia minora	Venous malformation	Venous malformation
TEK	c.2740C > T (p.Leu914Phe)	11	15/m	Soft tissue leg	Venous malformation	Veno-capillary malformation
TEK	c.2740C > T (p.Leu914Phe)	9	67/f	Upper lip	Venous lake	Combined malformation (extensive lymphatic component)
TEK	c.2690A > G (p.Tyr897Cys)	4	80/f	Subcutis	Unknown	Combined malformation (extensive lymphatic component)
TEK	c.2690A > G (p.Tyr897Cys)	4	9/f	Groin	Venous malformation, also anemia. d.d. Blue rubber bleb nevus.	Combined malformation (extensive lymphatic component)
TEK	c.2740C > T (p.Leu914Phe)	8	33/m	Lower arm	Venous malformation	Venous malformation
TEK	c.2740C > T (p.Leu914Phe)	5	17/f	Leg	Unknown	Veno-capillary malformation
TEK	c.2740C > T (p.Leu914Phe)	5	10/m	Lip	Venous malformation	Veno-capillary malformation
TEK	c.2740C > T (p.Leu914Phe)	9	15/m	Soft tissue arm	Unknown	Veno-capillary malformation
TEK	c.2689 T > C (p.Tyr897His)	12	2/m	Arm	Localized atypical tumor by ultra sound. d.d. vascular malformation	Veno-capillary malformation
GNAQ	c.548G > A (p.Arg183Gln)	7	56/f	Face	Port wine stain with hypertrophy	Venous malformation
KRAS	c.34G > T (p.Gly12Cys)	6	76/m	Lower leg	Arteriovenous malformation (AVM) with ulceration	AVM
KRAS	c.34G > T (p.Gly12Cys)	6	68/f	Finger	AVM	AVM
KRAS	c.35G > T (p.Gly12Val)	3	17/f	Brain	Unknown	Venous malformation
GNA11	c.626A > T (p.Gln209Leu)	9	45/m	Skin ear canal	Unknown	Veno-capillary malformation
PIK3CA; GNAQ	c.1624G > A (p.Gln542Lys); c.627A > C (p.Gln209His)	15; 13	27/m	Skin	High flow lesion, d.d. AVM	Veno-capillary malformation
PIK3CA; IDH1	c.1624G > A (p.Gln542Lys); c.394C > T (p.Arg132Cys)	24; 20	21/m	Subcutis leg	Atypical vascular lesion	SCH

Abbreviations: KTS, Klippel Trenaunay syndrome; AVM, arteriovenous malformation; SCH, spindle cell hemangioma.

a veno-capillary morphology. Of the 7 cases with a GNAQ mutation, 4 were veno-capillary malformations, 2 VMs, and 1 had combined features including an arterial component. The *AKT1* mutated case consisted of veins only. The 2 cases harboring an *IDH1* and *PIK3CA* mutation were SCHs. The other 4 cases with a *PIK3CA* mutation combined with either a GNA11 ($n = 2$) or GNAQ ($n = 2$) mutation were all veno-capillary malformations. Histology of the *RASA1* and *PTEN* mutated cases could not be determined due to anonymization.

In the prospective cohort ($n = 198/217$), mutations and the percentages of mutated cells within the histologically determined groups are shown in Supporting Information Table S5.

The spectrum of mutations per group was, based on clinical and histological features, relatively heterogeneous. The capillary malformations, for example, showed 3 GNAQ and 3 KRAS mutations, 1 NRAS and 1 PIK3CA mutation, and also a combined PIK3CA with GNA11 mutation. In AVMs (4 out of 17) and LMs (8 out of 14), without exception however, PIK3CA mutations were identified.

4 | DISCUSSION

Vascular malformations belonging to the spectrum of overgrowth syndromes are, in most cases, genetically characterized by somatic mosaic pathogenic hotspot mutations or, more rarely, by germline mutations.¹ We analyzed frequently mutated positions in more than 20 genes in clinically/radiologically and/or histopathologically diagnosed vascular malformations/overgrowth syndromes to gain more insight into their molecular biology linked to clinicopathological characteristics.

4.1 | Technical challenges for molecular diagnostics

The range of identified mutant allele frequencies shows that it is highly valuable to analyze vascular malformations with NGS, especially with the inclusion of UMIs allowing an analytical sensitivity of 1% variant allele frequency in sequence analyses of FFPE tissue. At least 65% of mutations would have been missed using Sanger sequencing, based on a detection

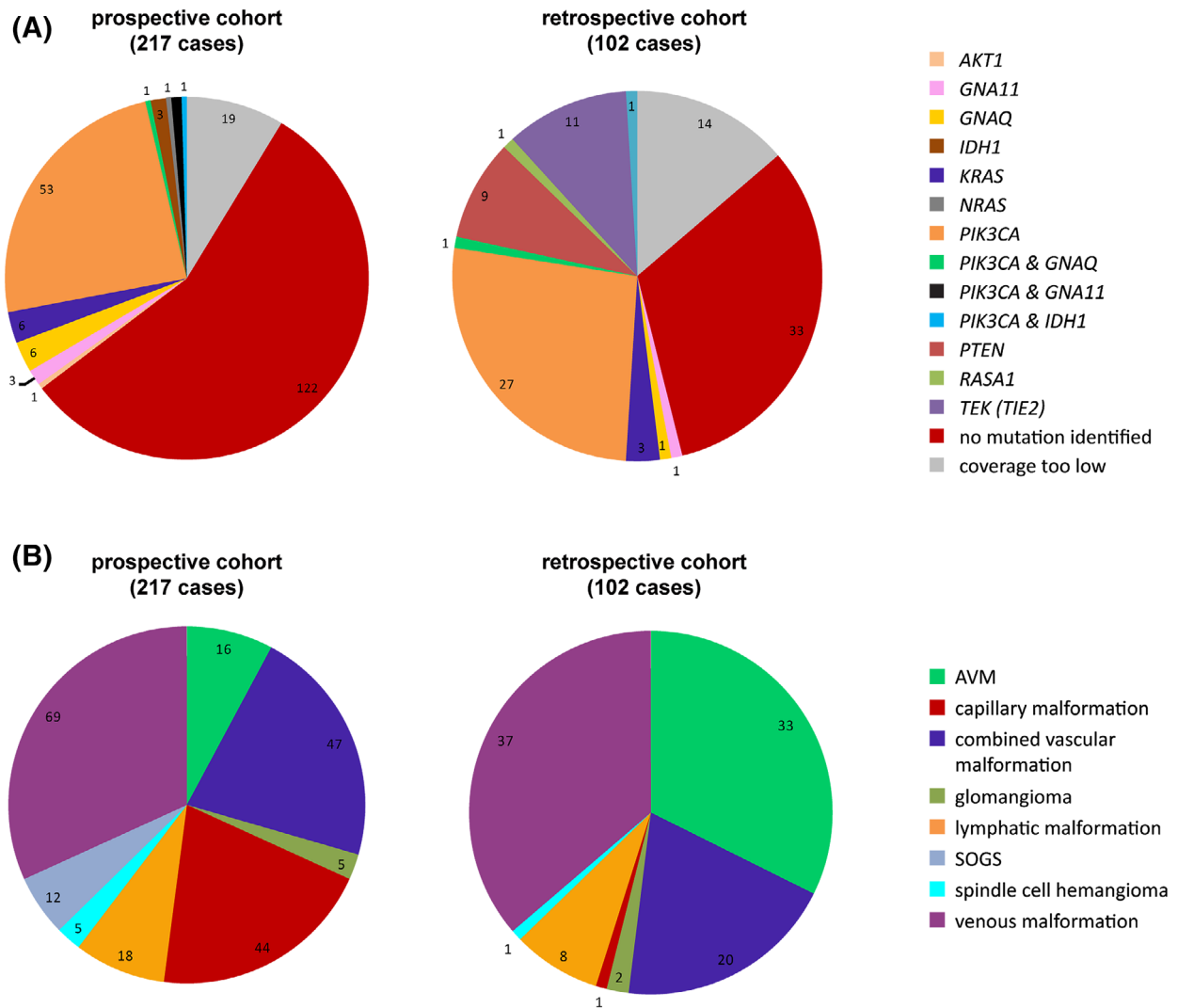


FIGURE 1 Overview of prospective and retrospective vascular malformation cohort. NGS-based sequence analyses of a total of 319 cases of vascular malformations was performed in a routine diagnostic (prospective) and retrospective cohort consisting of histologically confirmed vascular anomalies. Molecular results grouped per mutated gene (top) and the clinicopathological entities in both cohorts (bottom). Abbreviations: AVM, arteriovenous malformation; SOGS, somatic overgrowth syndrome

level of at least 10% mutant alleles. More sensitive techniques such as digital droplet PCR would potentially result in identification of more pathogenic mutations.²⁷ However, the variety of mutations in combination with limited amounts of affected cells and available tissue require an approach in which a larger number of positions can be tested simultaneously. The identified low frequency pathogenic variants are in line with the mosaicism.

The detection of mosaic mutations with variant allele frequencies <10% in gDNA from FFPE tissue depends on quality and quantity of isolated gDNA and the presence of cytosine deamination resulting in C:G > T:A mutations. False-negative calls can result from the overestimation of the actual number of analyzed DNA molecules and potential false-positive calls can arise from deamination artifacts.

4.2 | Vascular malformations span a mutational spectrum affecting multiple signaling pathways

4.2.1 | PI3K/AKT/mTOR pathway

Activating mutations in *PIK3CA*, *AKT1*, and *TEK*, and alternatively disrupting mutations in *PTEN*, activate the mTOR pathway, regulating cell

growth, proliferation, survival and cell cycle progression.^{2,6,28,29} *PIK3CA* mutations are the most ubiquitous ones in vascular malformations. This was reflected in our cohorts with ~30% ($n = 86$) of the cases being affected. They show a variable phenotype both histologically (LMs, VMs, and AVMs) and clinically (low flow malformations), which is in accordance with the literature.^{26,30} *AKT1* was mutated in only 1 case (~0.3%) of the retrospective cohort, showing a p.Glu17Lys mutation, the same mutation that has been most frequently described in the literature.¹² Mutations in *TEK/TIE2* with about 85% of cases harboring a p.[Leu914Phe] missense mutation results nearly exclusively in venous malformations.³¹⁻³³ In our retrospective cohort, 11 cases (12.5%) were mutated. A c.2740C > T (p.(Leu914Phe)) mutation was found in 7 of them. Other mutations we identified were c.2690A > G (p.[Tyr897Cys]) ($n = 3$) and c.2689 T > C (p.[Tyr897His]) ($n = 1$) indicating that only screening of p.(Leu914Phe) is insufficient. Clinically, all cases had a venous phenotype including 1 case with a BRBN syndrome. Both *TEK* mutations found in the BRBN case were present in *cis*. As all mutated reads contained both mutations, the same variant allele frequency was suggested.³⁴ In contrast to the

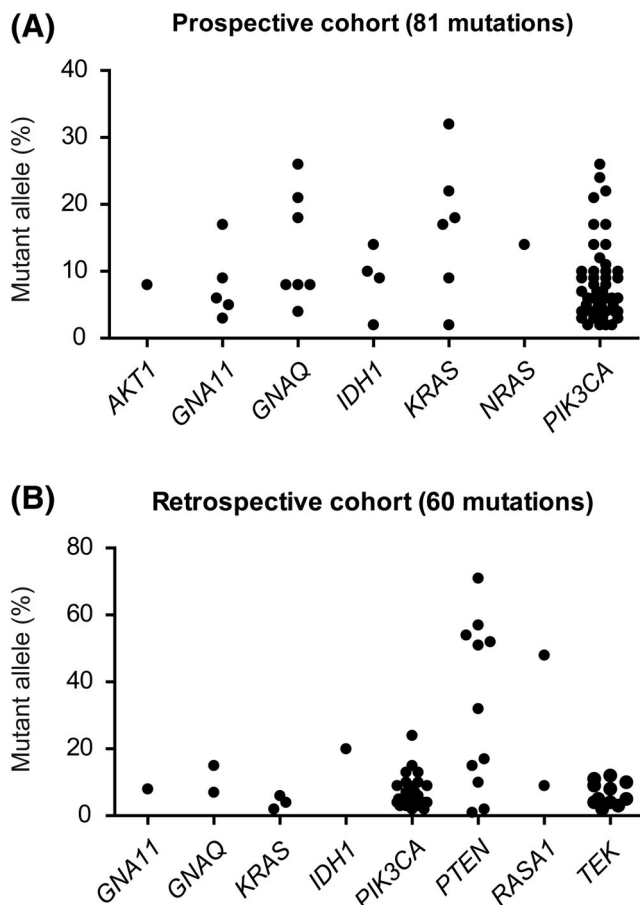


FIGURE 2 Mutant allele frequencies of identified mutations. The mutant allele frequencies of all (likely) pathogenic mutations in both, the prospective (top) and retrospective (bottom) cohort, grouped per gene

literature,^{31–33} our *TEK* mutated cases were histologically more heterogeneous showing also combined lesions with a venous, capillary, and/or a lymphatic component.

The retrospective cohort contained 9 *PTEN* mutated cases (~10%) (see later), adding up to a total of 107 cases containing mutations indicative of mTOR activation in the PI3K/AKT/mTOR pathway.

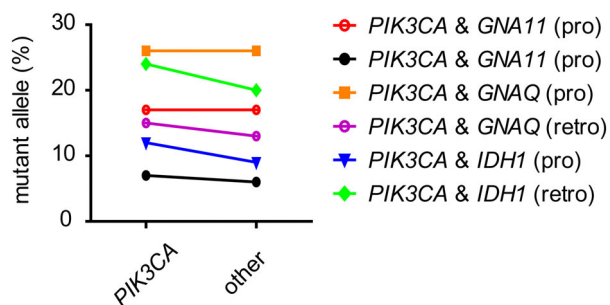


FIGURE 3 Mutant allele frequencies in cases with two pathogenic hotspot mutations. In 6 cases, a combination of one *PIK3CA* with an additional pathogenic activating (*GNA11* and *GNAQ*) or transforming (*IDH1*) hotspot mutation was identified. The mutant allele frequencies of both mutations are depicted and connected per case

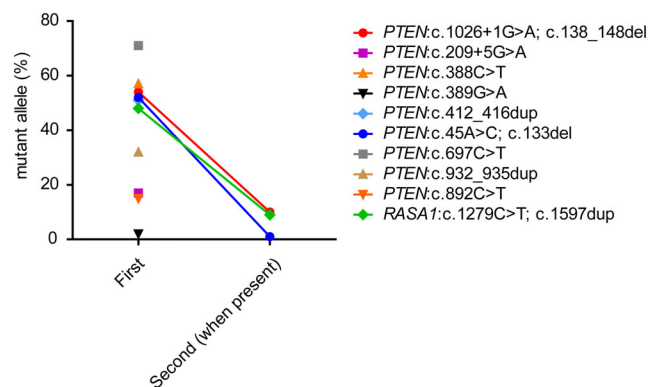


FIGURE 4 Mutant allele frequencies in cases with disrupting mutations. In 10 cases of the retrospective cohort, disrupting mutations were identified in *PTEN* (9 cases) and *RASA1* (1 case). In a subset of cases, an additional mutation was found. The mutant allele frequencies are depicted per case, with connected data points in case two mutations were identified

4.2.2 | RAS-RAF-MEK-ERK signaling pathway

RAS signaling can be stimulated by both activating (somatic) mutations in *KRAS*, *HRAS*, *NRAS* as well as inactivating (germline) mutations in *RASA1*, which is a RAS-GAP (Guanine Activating Protein) and negative regulator of the RAS-RAF-MEK-ERK signaling pathway. Subsequently, diverse cellular signaling networks including the mTOR and ERK pathways are activated.³⁵ Histologically, in contrast with the heterogeneity seen for the other mutations, 8 out of 11 RAS mutated vascular malformations were well-circumscribed (capillary and/or venous), while lesions with other mutations were almost all noncircumscribed.

GNAQ is a gene encoding guanine nucleotide binding protein G(q) alpha, a subunit within a complex that hydrolyses the intracellular messenger GTP to GDP.³⁶ *GNA11* and *GNA14* are analogous binding proteins with nearly the same protein sequence as *GNAQ*.^{18,36} When mutated, these genes induce changes in cellular morphology and cell growth by upregulation of mainly the RAS-RAF-MEK-ERK pathway.¹⁸

Combining the two cohorts, we detected 9 *KRAS*, 1 *NRAS*, 7 *GNAQ*, and 4 *GNA11* hotspot mutations; *GNAQ* and *GNA11* were in 2 cases each combined with a *PIK3CA* mutation. These, and one inactivating mutation in *RASA1*, suggest a more significant role (about 8% of all the included cases) of the RAS-RAF-MEK-ERK pathway in vascular malformations than may be expected from the literature.^{15,16}

We did not detect *GNA14* mutations. This is in accordance with the literature reporting that such mutations are restricted to tufted hemangioma and kaposiform hemangioendothelioma, which were not included in our cohorts.²²

4.3 | IDH 1/2 mutated vascular lesions are malformations rather than tumors

Five cases showed an *IDH1* mutation, in two cases in combination with a *PIK3CA* mutation (one of these cases was included in a previously published cohort³⁷). Isocitrate dehydrogenases (*IDH*) are metabolic enzymes which, as a result of a somatic mutation (in both *IDH1* and *IDH2*), mostly inhibit the catalyzation of isocitrate to α -ketoglutarate

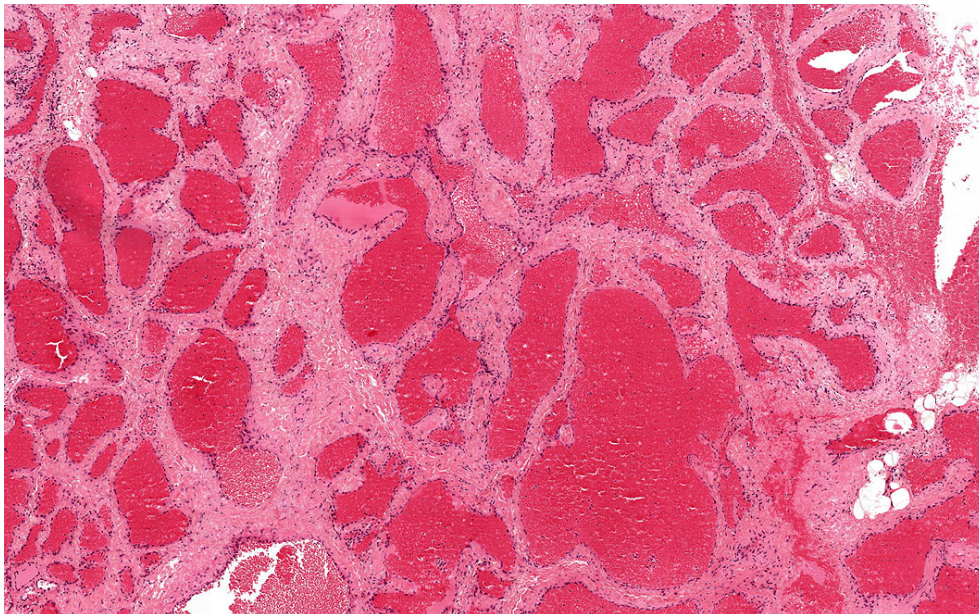


FIGURE 5 Venous/cavernous malformation. HE, $\times 100$ [Color figure can be viewed at wileyonlinelibrary.com]

(α -KG). This results in aberrant DNA methylation and histone modification leading to stabilization of hypoxia inducible factor-1 α subsequently inducing angiogenesis.³⁸ Four of our cases were spindle cell hemangiomas (SCH), in line with previous findings.³⁷ Interestingly, the fifth lesion was a small biopsy of an intramuscular veno-capillary malformation without a spindle cell component. Vice versa, we also found a SCH with only a *PIK3CA* mutation (17% variant allele frequency) confirming that SCHs belong to the heterogeneous spectrum of vascular malformations rather than to vascular tumors.^{4,37}

4.4 | Combined mutations

In 6 cases we identified a combination of an activating mutation in *PIK3CA* with an additional pathogenic mutation in *GNAQ*, *GNA11*, or

IDH1. As these cases had a heterogeneous/combined phenotype without specific clinical symptoms, no conclusion can be drawn regarding the significance of the dominant mutation.

To our knowledge, such a combination of mutations in two individual genes in vascular malformations/overgrowth syndromes has not been reported before. It is likely that this can be explained by the presence of two related events in the same cells, because in all cases the mutant allele frequencies of both mutations were very similar. However, an *in situ* approach would be required to formally prove this concept. From a signaling perspective, the pathogenic mutations in *GNAQ*, *GNA11*, and *IDH1* are expected to provide additional growth advantage in parallel with *PIK3CA*-driven mTOR activation. One could argue that different pathways in parallel are involved in aberrant development of vascular structures and other

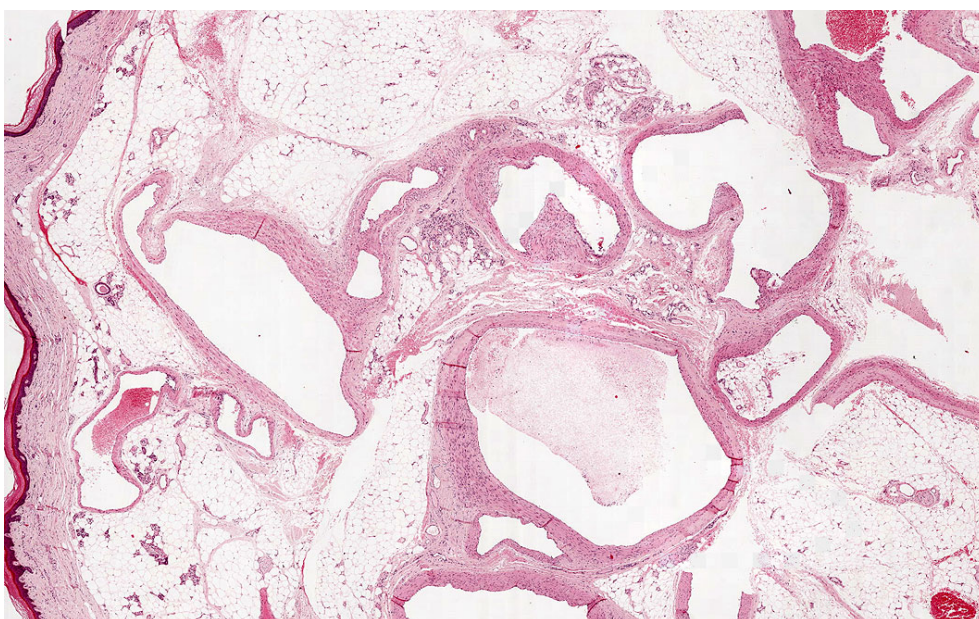


FIGURE 6 Arteriovenous malformation showing variation in wall thickness. HE, $\times 20$ [Color figure can be viewed at wileyonlinelibrary.com]

affected tissue. This may be relevant information if application of targeted treatments is considered.

4.5 | Potential germline aberrations in cases of vascular anomalies

Pathogenic germline mutations in *PTEN* lead to *PTEN* hamartoma tumor syndrome (PHTS) with susceptibility to multiple tumors as well as vascular malformations. This process is initiated after loss or inactivation of the second (wild type) allele by somatic mutation resulting in increased levels of PIP3 and increased activation of *AKT*.²⁹ We found 9 cases (approximately 10% of the cases) with a (likely) pathogenic *PTEN* mutation, of which at least 4 were a germline mutation, in the retrospective cohort. This unexpectedly high percentage of *PTEN* mutations suggests a much more important role in the etiology of sporadic vascular malformations than anticipated, as *PTEN*-associated anomalies are only described in the context of PHTS.^{29,39}

We also identified 1 case with a potential germline *RASA1* mutation. Because data from our retrospective cohort were analyzed anonymously, we could not associate the *PTEN* and *RASA1* positive lesions to individual histological and clinical characteristics. However, a vascular malformation may well represent the first clinical presentation of an eventually more extensive syndromal phenotype, which is especially relevant in the context of de novo germline mutations or atypical phenotypic presentation. Our findings urge for clinical awareness of this potentially unrecognized patient group of vascular malformations at risk for germline-associated tumors.

Complete analyses of all coding and splice site sequences is required to identify all disrupting mutations, in contrast to the aforementioned “hotspot” analyses; this is challenging when using relatively poor quality gDNA obtained from FFPE tissue. Due to limitations in horizontal and vertical coverage for *ACVRL1*, *ENG*, and *GLMN*, but also *PTEN* and *RASA1*, pathogenic disruptions in these genes may have been remained undetected.

4.6 | Therapeutic opportunities for vascular malformations

There is increasing evidence^{28,40} that sirolimus, an mTOR inhibitor, can be used to treat a subset of the vascular malformations with a more favorable balance between effect and side effects than conventional treatments like surgery, embolization, or laser therapy.⁴¹ The precise mechanism behind this treatment is still unknown, but at least 107 of 286 cases in our series harbored mutations predicted to activate mTOR signaling. These mTOR activating cases are not limited to *PIK3CA*, so a more comprehensive analysis including additional genes involved in this pathway could increase the diagnostic and therapeutic yield (in our set-up by ~25%). Similarly, MEK inhibitors seem to be a promising therapeutic agent for lesions harboring mutations involved in the RAS-RAF-MEK-ERK pathway¹⁶; such mutations were found in 25 of our cases. The mapping of causative and druggable mutations by sequencing appears to be a big promise for patients with hitherto hardly treatable conditions in the vascular anomalies spectrum. Clinical trials with sirolimus with favorable initial results exemplify the potency of this new medical approach.^{42,43}

5 | CONCLUSION

In summary, mutational analysis of vascular malformations is of high diagnostic value and an indispensable addition to regular diagnostics, because clinical, radiological, and pathological investigations often offer insufficient clarity. Furthermore, it can provide clues for an underlying hereditary condition due to a germline mutation. In addition, increased knowledge of pathogenic mutations present in these lesions can stratify patients for targeted therapeutic options.^{15,40,44} A comprehensive and sensitive analysis is required because of the spectrum of genes involved and the mosaicism with low levels of mutated cells and also combined mutations.

ACKNOWLEDGMENTS

We thank all technicians of the Molecular Diagnostic Group, especially Annemiek Kastner-van Raaij and Sandra Hendriks-Cornelissen and other members of the Genome Technology Unit, Laboratory of Tumor Genetics, Departments of Pathology and Genetics, especially Arjen Mensenkamp.

CONFLICT OF INTEREST

Authors have no disclosures/conflict of interest.

ORCID

Roel W. Ten Broek  <https://orcid.org/0000-0001-7467-5818>

Uta Flucke  <https://orcid.org/0000-0003-0315-4307>

REFERENCES

- Blei F. Overgrowth syndromes with vascular anomalies. *Curr Probl Pediatr Adolesc Health Care*. 2015;45(4):118-131.
- Keppeler-Noreuil KM, Rios JJ, Parker VE, et al. PIK3CA-related overgrowth spectrum (PROS): diagnostic and testing eligibility criteria, differential diagnosis, and evaluation. *Am J Med Genet A*. 2015;167A(2):287-295.
- Keppeler-Noreuil KM, Sapp JC, Lindhurst MJ, et al. Clinical delineation and natural history of the PIK3CA-related overgrowth spectrum. *Am J Med Genet A*. 2014;164A(7):1713-1733.
- Wassef M, Blei F, Adams D, et al. Vascular Anomalies Classification: Recommendations From the International Society for the Study of Vascular Anomalies. *Pediatrics*. 2015;136(1):e203-e214.
- Happle R. Mosaicism in human skin. Understanding the patterns and mechanisms. *Arch Dermatol*. 1993;129(11):1460-1470.
- Freed D, Stevens EL, Pevsner J. Somatic mosaicism in the human genome. *Genes (Basel)*. 2014;5(4):1064-1094.
- Uller W, Fishman SJ, Alomari AI. Overgrowth syndromes with complex vascular anomalies. *Semin Pediatr Surg*. 2014;23(4):208-215.
- Boon LM, Ballieux F, Vikkula M. Pathogenesis of vascular anomalies. *Clin Plast Surg*. 2011;38(1):7-19.
- Uebelhoefer M, Boon LM, Vikkula M. Vascular anomalies: from genetics toward models for therapeutic trials. *Cold Spring Harb Perspect Med*. 2012;2(8):a009688.
- Vahidnezhad H, Youssefian L, Uitto J. Klippel-Trenaunay syndrome belongs to the PIK3CA-related overgrowth spectrum (PROS). *Exp Dermatol*. 2016;25(1):17-19.
- Kang HC, Baek ST, Song S, Gleeson JG. Clinical and Genetic Aspects of the Segmental Overgrowth Spectrum Due to Somatic Mutations in PIK3CA. *J Pediatr*. 2015;167(5):957-962.

12. Lindhurst MJ, Sapp JC, Teer JK, et al. A mosaic activating mutation in AKT1 associated with the Proteus syndrome. *N Engl J Med*. 2011;365(7):611-619.
13. Shirley MD, Tang H, Gallione CJ, et al. Sturge-Weber syndrome and port-wine stains caused by somatic mutation in GNAQ. *N Engl J Med*. 2013;368(21):1971-1979.
14. Amary MF, Damato S, Halai D, et al. Ollier disease and Maffucci syndrome are caused by somatic mosaic mutations of IDH1 and IDH2. *Nat Genet*. 2011;43(12):1262-1265.
15. Al-Olabi L, Polubothu S, Dowsett K, et al. Mosaic RAS/MAPK variants cause sporadic vascular malformations which respond to targeted therapy. *J Clin Invest*. 2018;128:5185.
16. Nikolaev SI, Vetiska S, Bonilla X, et al. Somatic activating KRAS mutations in arteriovenous malformations of the brain. *N Engl J Med*. 2018;378(3):250-261.
17. Brouillard P, Boon LM, Mulliken JB, et al. Mutations in a novel factor, glomulin, are responsible for glomuvenous malformations ("glomangiomas"). *Am J Hum Genet*. 2002;70(4):866-874.
18. Lim YH, Bacchicocchi A, Qiu J, et al. GNA14 somatic mutation causes congenital and sporadic vascular tumors by MAPK activation. *Am J Hum Genet*. 2016;99(2):443-450.
19. McDonald J, Wooderchak-Donahue W, VanSant Webb C, Whitehead K, Stevenson DA, Bayrak-Toydemir P. Hereditary hemorrhagic telangiectasia: genetics and molecular diagnostics in a new era. *Front Genet*. 2015;6:1.
20. Revencu N, Boon LM, Mendola A, et al. RASA1 mutations and associated phenotypes in 68 families with capillary malformation-arteriovenous malformation. *Hum Mutat*. 2013;34(12):1632-1641.
21. Nozaki T, Nosaka S, Miyazaki O, et al. Syndromes associated with vascular tumors and malformations: a pictorial review. *Radiographics*. 2013;33(1):175-195.
22. Tan WH, Baris HN, Burrows PE, et al. The spectrum of vascular anomalies in patients with PTEN mutations: implications for diagnosis and management. *J Med Genet*. 2007;44(9):594-602.
23. de Leng WW, Gadellaa-van Hooijdonk CG, Barendregt-Smouter FA, et al. Targeted next generation sequencing as a reliable diagnostic assay for the detection of somatic mutations in tumours using minimal DNA amounts from formalin fixed paraffin embedded material. *PLoS one*. 2016;11(2):e0149405.
24. Eijkelenboom A, Kamping EJ, Kastner-van Raaij AW, et al. Reliable Next-Generation sequencing of Formalin-Fixed, Paraffin-Embedded tissue using single molecule tags. *J Mol Diagn*. 2016;18(6):851-863.
25. Kurek KC, Luks VL, Ayturk UM, et al. Somatic mosaic activating mutations in PIK3CA cause CLOVES syndrome. *Am J Hum Genet*. 2012;90(6):1108-1115.
26. Luks VL, Kamitaki N, Vivero MP, et al. Lymphatic and other vascular malformative/overgrowth disorders are caused by somatic mutations in PIK3CA. *J Pediatr*. 2015;166(4):1048-1054. e1041-1045.
27. Salk JJ, Schmitt MW, Loeb LA. Enhancing the accuracy of next-generation sequencing for detecting rare and subclonal mutations. *Nat Rev Genet*. 2018;19(5):269-285.
28. Boscolo E, Limaye N, Huang L, et al. Rapamycin improves TIE2-mutated venous malformation in murine model and human subjects. *J Clin Invest*. 2015;125(9):3491-3504.
29. Nathan N, Keppler-Noreuil KM, Biesecker LG, Moss J, Darling TN. Mosaic disorders of the PI3K/PTEN/AKT/TSC/mTORC1 signaling pathway. *Dermatol Clin*. 2017;35(1):51-60.
30. Limaye N, Kangas J, Mendola A, et al. Somatic activating PIK3CA mutations cause venous malformation. *Am J Hum Genet*. 2015;97(6):914-921.
31. Du Z, Zheng J, Zhang Z, Wang Y. Review of the endothelial pathogenic mechanism of TIE2-related venous malformation. *J Vasc Surg Venous Lymphat Disord*. 2017;5(5):740-748.
32. Soblet J, Limaye N, Uebelhoefer M, Boon LM, Vikkula M. Variable Somatic TIE2 Mutations in Half of Sporadic Venous Malformations. *Mol Syndromol*. 2013;4(4):179-183.
33. Uebelhoefer M, Natynki M, Kangas J, et al. Venous malformation-causative TIE2 mutations mediate an AKT-dependent decrease in PDGFB. *Hum Mol Genet*. 2013;22(17):3438-3448.
34. Soblet J, Kangas J, Natynki M, et al. Blue rubber bleb nevus (BRBN) syndrome is caused by somatic tek (TIE2) mutations. *J Invest Dermatol*. 2017;137(1):207-216.
35. Simanshu DK, Nissley DV, McCormick F. RAS proteins and their regulators in human disease. *Cell*. 2017;170(1):17-33.
36. Ayturk UM, Couto JA, Hann S, et al. Somatic activating mutations in GNAQ and GNA11 are associated with congenital hemangioma. *Am J Hum Genet*. 2016;98(4):789-795.
37. Ten Broek RW, Bekers EM, de Leng WWJ, et al. Mutational analysis using Sanger and next generation sequencing in sporadic spindle cell hemangiomas: A study of 19 cases. *Genes Chromosomes Cancer*. 2017;56(12):855-860.
38. Schaap FG, French PJ, Bovee JV. Mutations in the isocitrate dehydrogenase genes IDH1 and IDH2 in tumors. *Adv Anat Pathol*. 2013;20(1):32-38.
39. Mester J, Charis E. PTEN hamartoma tumor syndrome. *Handb Clin Neurol*. 2015;132:129-137.
40. Triana P, Dore M, Cerezo VN, et al. Sirolimus in the treatment of vascular anomalies. *Eur J Pediatr Surg*. 2017;27(1):86-90.
41. Hammill AM, Wentzel M, Gupta A, et al. Sirolimus for the treatment of complicated vascular anomalies in children. *Pediatr Blood Cancer*. 2011;57(6):1018-1024.
42. Adams DM, Trenor CC 3rd, Hammill AM, et al. Efficacy and safety of sirolimus in the treatment of complicated vascular anomalies. *Pediatrics*. 2016;137(2):e20153257.
43. Hammer J, Seront E, Duez S, et al. Sirolimus is efficacious in treatment for extensive and/or complex slow-flow vascular malformations: a monocentric prospective phase II study. *Orphanet J Rare Dis*. 2018;13(1):191.
44. Ranieri C, Di Tommaso S, Loconte DC, et al. In vitro efficacy of ARQ 092, an allosteric AKT inhibitor, on primary fibroblast cells derived from patients with PIK3CA-related overgrowth spectrum (PROS). *Neurogenetics*. 2018;19:77-91.

SUPPORTING INFORMATION

Additional supporting information may be found online in the Supporting Information section at the end of the article.

How to cite this article: Ten Broek RW, Eijkelenboom A, van der Vleuten CJM, et al. Comprehensive molecular and clinicopathological analysis of vascular malformations: A study of 319 cases. *Genes Chromosomes Cancer*. 2019;58:541-550. <https://doi.org/10.1002/gcc.22739>